Aust. J. Phys., 1981, **34**, 627–38

A Collective Model Description of the Dipole States in the Even–Even $N = 28$ Isotones

J. Weise

School of Physics, University of Melbourne, Parkville, Vic. 3052.

Abstract

The photoabsorption and photon scattering cross sections for the even–even ($N = 28$) isotones ^{50}Ti, ^{52}Cr and ^{54}Fe are calculated within the framework of the Gneuss–Greiner model and in the light of recent data.

1. Introduction

Shell model calculations, predominantly using $(1f^{n}_{7/2})$ configurations with small admixtures of $(1f^{n-1}_{7/2}\,2p_{3/2})$ and $(1f^{n-1}_{7/2}\,1f_{5/2})$ components with an inert ^{48}Ca core, have been successful in predicting some of the properties of the even–even $N = 28$ isotones (Lips and McEllistrem 1970; Saayman and Irvine 1976). Although such calculated spectra compare exceptionally well with the data, the 0^+_2 levels are predicted much too high in energy, particularly for ^{52}Cr where, in addition, the E2 transition strengths of decays from the 4^+_1 and 2^+_2 states are too low. Lips (1971) concluded that the configuration mixing already introduced was not sufficient to account for the core deformation (most severe in the middle of the shell and noticeable in predicting the energies of excited 0^+ states) and that neutron excitations outside the $f_{7/2}$ shell may be of importance. A shell model calculation for ^{54}Fe involving basis configurations of the type $(f^{m}_{7/2}p^{n}_{3/2}p^{s}_{1/2})$, $m \geqslant 12$ and $s = 0, 1$, by Amos *et al.* (1978) revealed that both the 2^+_1 and 4^+_1 state excitations proceed mainly, relative to an inert ^{40}Ca core, by an $f_{7/2}$ proton transition and the 2^+_2 state by an $f_{7/2}$ to $p_{3/2}$ neutron transition. Furthermore, with the introduction of such neutron transitions, Morrison *et al.* (1975) and Pronko *et al.* (1974) were able to reproduce satisfactorily the positions of the low-lying 0^+ levels in ^{54}Fe and ^{50}Ti respectively.

To describe adequately just a few features of the low-lying properties of these nuclei, it was necessary to introduce excitations outside the ^{48}Ca core. A microscopic description of the giant dipole resonance (GDR) region in this basis, although desirable, would therefore be extremely difficult. A much simpler approach, which is followed here, is that of the dynamic collective model (DCM) or, in particular, its development to the model of Gneuss and Greiner (1971, and references therein), whereby a description of the collective properties of nuclei between the two extremes of vibrator and rotator is possible. Only collective quadrupole degrees of freedom, which are nevertheless believed to dominate the low energy properties of even–even nuclei, are considered. The low energy parameters of the Hamiltonian of this model are derived by fitting as faithfully as possible a number of low energy features. The low energy collective degrees of freedom thus obtained are then coupled to the density vibrations of the GDR to predict the structure in the GDR region. A similar approach based on the interacting boson approximation (IBA) (Morrison and Weise 1981) would also suffice.

2. Theory

For completeness the model of Gneuss and Greiner (1971), extended by Rezwani *et al.* (1970, 1972) into the GDR region, is outlined together with the relevant equations necessary for the calculations presented in the next section. The total Hamiltonian is given by

$$H = H_{\mathrm{Q}}+H_{\mathrm{D}}+H_{\mathrm{DQ}}, \tag{1}$$

where H_{Q} describes the low energy quadrupole degrees of freedom,

$$\begin{aligned} H_{\mathrm{Q}} &= P_2[\pi^{[2]}\times\pi^{[2]}]^{[0]} + P_3[\pi^{[2]}\times\alpha^{[2]}\times\pi^{[2]}]^{[0]} \\ &\quad + C_2 L_2 + C_3 L_3 + C_4 L_2^2 + C_5 L_2 L_3 + C_6 L_3^2 + D_6 L_2^3; \qquad (2) \\ L_2 &= [\alpha^{[2]}\times\alpha^{[2]}]^{[0]}, \qquad L_3 = [\alpha^{[2]}\times\alpha^{[2]}\times\alpha^{[2]}]^{[0]}; \end{aligned}$$

H_{D} is the Hamiltonian of the GDR defined in terms of creation and annihilation operators $q_\nu^{[1]\dagger}$ and $q_\nu^{[1]}$ respectively for dipole phonons of unperturbed energy $\hbar\omega_1$, namely

$$H_{\mathrm{D}} = -3^{\frac{1}{2}}\hbar\omega_1[q^{[1]\dagger}\times q^{[1]}]^{[0]}; \tag{3}$$

and H_{DQ} is the interaction term between the dipole and quadrupole degrees of freedom,

$$\begin{aligned} H_{\mathrm{DQ}} &= \hbar\omega_1 B_1[q^{[1]\dagger}\times q^{[1]}\times\alpha^{[2]}]^{[0]} \\ &\quad + \hbar\omega_1 \sum_{j=0,2} B_{2j}[q^{[1]\dagger}\times q^{[1]}\times[\alpha^{[2]}\times\alpha^{[2]}]^{[j]}]^{[0]}, \end{aligned} \tag{4}$$

where the coupling constants B_1, B_{20} and B_{22} are determined uniquely from a hydrodynamical model. In equation (2), $\alpha_\mu^{[2]}$ and $\pi_\mu^{[2]}$ are the quadrupole collective coordinates and momenta describing the low energy states. The inertia parameters C_2, C_3, C_4, C_5, C_6 and D_6 determine the shape of the potential energy surface (PES) and hence the low energy properties, whilst the constants P_2 and P_3 in the kinetic energy part are respectively the harmonic and anharmonic mass parameters. The PES are obtained explicitly by expressing the collective potential energy in the intrinsic system of coordinates (β and γ), namely

$$\begin{aligned} V(\beta,\gamma) &= C_2(\tfrac{1}{5})^{\frac{1}{2}}\beta^2 - C_3(\tfrac{2}{35})^{\frac{1}{2}}\beta^3\cos 3\gamma + C_4\tfrac{1}{5}\beta^4 \\ &\quad - C_5(\tfrac{2}{175})^{\frac{1}{2}}\beta^5\cos 3\gamma + C_6\tfrac{2}{35}\beta^6\cos^2 3\gamma + D_6(\tfrac{1}{5})^{\frac{3}{2}}\beta^6. \end{aligned} \tag{5}$$

The model Hamiltonian of equation (2) can be diagonalized using as a basis a large number of eigenstates of the five-dimensional harmonic oscillator. The resultant eigenstates of this Hamiltonian, classified by their angular momentum l and z projection m, will be linear combinations of these basis states, namely

$$|\gamma, lm\rangle = \sum_{N\nu\alpha} C^\gamma(N\nu l\alpha)\,|[N]\nu l\alpha m\rangle. \tag{6}$$

The quadrupole moment of a nucleus in any such state and the reduced E2 transition probability between an initial state $|\gamma, lm\rangle$ and a final state $|\gamma', l'm'\rangle$ are defined in terms of the matrix elements of the quadrupole operator $Q^{[2]}$ by

$$Q(\gamma, lm{=}l) = \left(\frac{16\pi}{5}\right)^{\frac{1}{2}} \begin{pmatrix} l & 2 & l \\ -l & 0 & l \end{pmatrix} \langle \gamma, l \| Q^{[2]} \| \gamma, l \rangle, \tag{7a}$$

$$B(\mathrm{E2}: \gamma, l \to \gamma', l') = (2l+1)^{-1} |\langle \gamma', l' \| Q^{[2]} \| \gamma, l \rangle|^2, \tag{7b}$$

where the quadrupole operator is defined for a homogeneous charge distribution ρ_0, whence to second order in α,

$$\begin{aligned} Q_{2\mu} &= \int \rho(r)\, r^2\, \mathrm{Y}_{2\mu}\, \mathrm{d}\tau \\ &= \rho_0\, R_0^5 \{\alpha_{2\mu} - 10(70\pi)^{-\frac{1}{2}} [\alpha^{[2]} \times \alpha^{[2]}]_\mu^{[2]}\}. \end{aligned} \tag{8}$$

The diagonalization of the energy matrix for each of the angular momenta 0, 2, 3, 4, 5, 6 yields the energy levels and eigenstates. These eigenstates are then used to calculate the quadrupole moments and transition probabilities.

The eigenstates of the Hamiltonian H of (1) can be expanded in terms of product states of the five-dimensional quadrupole oscillator and the three-dimensional dipole oscillator, namely

$$H\,|n, I{=}1, M\rangle = E_n\,|n, I{=}1, M\rangle, \tag{9a}$$

$$|n, I{=}1, M\rangle = \sum_{N\nu\alpha l} C^n(N\nu\alpha l)\,(lm1m' \mid 1M)\,|[N]\nu l\alpha m\rangle_{\mathrm{Q}}\,|[1]1m'\rangle_{\mathrm{D}}, \tag{9b}$$

where the quadrupole states with angular momenta 0, 2 are as defined in equation (6) and

$$|[1]1m'\rangle_{\mathrm{D}} = q_{m'}^\dagger\,|0\rangle.$$

To determine the dipole strengths, the dipole operator must be expressed in terms of the collective coordinates, namely

$$\begin{aligned} D^{[1]} = M_0\{&q^{[1]\dagger} + q^{[1]} + M_1[(q^{[1]\dagger} + q^{[1]}) \times \alpha^{[2]}]^{[1]} \\ &+ \sum_{j=0,2} M_{2j}[(q^{[1]\dagger} + q^{[1]}) \times (\alpha^{[2]} \times \alpha^{[2]})^{[j]}]^{[1]}\}, \end{aligned} \tag{10}$$

where $M_0 = 0{\cdot}654\hbar\{NZ(1+\alpha)/AM\hbar\omega_1\}^{\frac{1}{2}}$, $M_1 = -0{\cdot}554$, $M_{20} = 0{\cdot}011$, $M_{22} = 0{\cdot}100$, and α is the effective-mass parameter.

From this model, a number of physical quantities in the GDR region can be calculated:

(*a*) The total γ-ray absorption cross section

$$\sigma(E) = \frac{8\pi}{3}\frac{e^2}{\hbar c}\sum_n |\langle n, I{=}1 \| D \| 0\rangle|^2 \frac{E_n \Gamma_n}{(E^2 - E_n^2)^2/E^2 + \Gamma_n^2}, \tag{11}$$

where E_n and Γ_n are the energies and widths respectively of the GDR states $|n, I{=}1, M\rangle$, and $|0\rangle$ represents the ground states of H_{D} and H_{Q}.

(*b*) The γ-ray scattering cross section

$$\mathrm{d}\sigma_{0^+\to I_f}(E,\theta)/\mathrm{d}\Omega = (E'/E)\,|\,P_{I_f}|^2 g_{I_f}(\theta)\,, \tag{12}$$

where the angular distributions are

$$g_0 = \tfrac{1}{6}(1+\cos^2\theta)\,, \quad g_1 = \tfrac{1}{4}(2+\sin^2\theta)\,, \quad g_2 = \tfrac{1}{12}(13+\cos^2\theta)\,, \tag{13}$$

θ is the scattering angle, and E and E' are the energies of the incident and scattered photons respectively. The polarizabilities are

$$P_{I_f} = \frac{1}{\{3(2I_f+1)\}^{\frac{1}{2}}}\frac{EE'}{(\hbar c)^2}\sum_n \langle I_f\,||\,D^{[1]}\,||\,1_n\rangle\langle 1_n\,||\,D^{[1]}\,||\,0\rangle$$
$$\times\left(\frac{1}{E_n+E'+\frac{1}{2}\mathrm{i}\Gamma_n}+\frac{(-)^j}{E_n-E-\frac{1}{2}\mathrm{i}\Gamma_n}\right)-\frac{\delta_{I_f0}\,3^{\frac{1}{2}}(Ze)^2}{AMc^2}\,, \tag{14}$$

where $|\,1_n\rangle \equiv |\,n,I=1\rangle$.

(*c*) The dipole sum rule

$$\mathrm{DSR} = \hbar\omega_1\,M_0^2(1+n_0+n_2\langle L_2\rangle)\,, \tag{15}$$

where $n_0 = \hbar^2 P_2\,M_1^2/\hbar\omega_1 = 0\cdot307\,\hbar P_2/\omega_1$ and $n_2 = n_2' + (\frac{4}{5}\hbar^2 P_2/\hbar\omega_1)(M_{20}^2+M_{22}^2) = -0\cdot133 + 0\cdot81\times10^{-2}\hbar P_2/\omega_1$, with the expectation value of L_2 taken from the ground state. This dipole sum rule is essentially equivalent to the classical estimate $60NZ/A$ and provides a means of evaluating the contribution from the interaction H_{DQ}, since the first term in (15) represents the dipole sum if H_{DQ} vanishes and amounts to 86% of the classical dipole sum.

Table 1. Low energy parameters of ^{50}Ti, ^{52}Cr and ^{54}Fe used in present calculation

Mass parameters P_2 and P_3 are in units of $10^{40}(\mathrm{MeV\,s^2})^{-1}$, the stiffness parameters $C_2, C_3, C_4, C_5, C_6, D_6$ in MeV

Nucleus	^{50}Ti	^{52}Cr	^{54}Fe
P_2	5·44	10·73	6·49
P_3	0·0	0·0	−7·40
C_2	−24·10	91·73	134·38
C_3	917·78	0·0	0·0
C_4	5183·30	−443·53	−879·32
C_5	51730·30	124·77	287·77
C_6	364693·59	0·0	0·0
D_6	53586·60	778·01	2087·48

3. Discussion and Conclusions

The low energy parameters of Rebel and Habs (1973) and Sedlmayr (1976) used in the present calculation are given in Table 1. The PES obtained from the inertia parameters of Table 1 are presented in Fig. 1 for ^{50}Ti, ^{52}Cr and ^{54}Fe. The necessity to introduce excitations from the $N = 28$ neutron core to account appropriately for the energies of the 0_2^+ states, and the enhancement (over single particle estimates) of certain transition rates, implies that deformation effects are important in these nuclei. Indeed, the slight prolate axial symmetries in the PES of otherwise spherical vibrators are clear evidence of these effects.

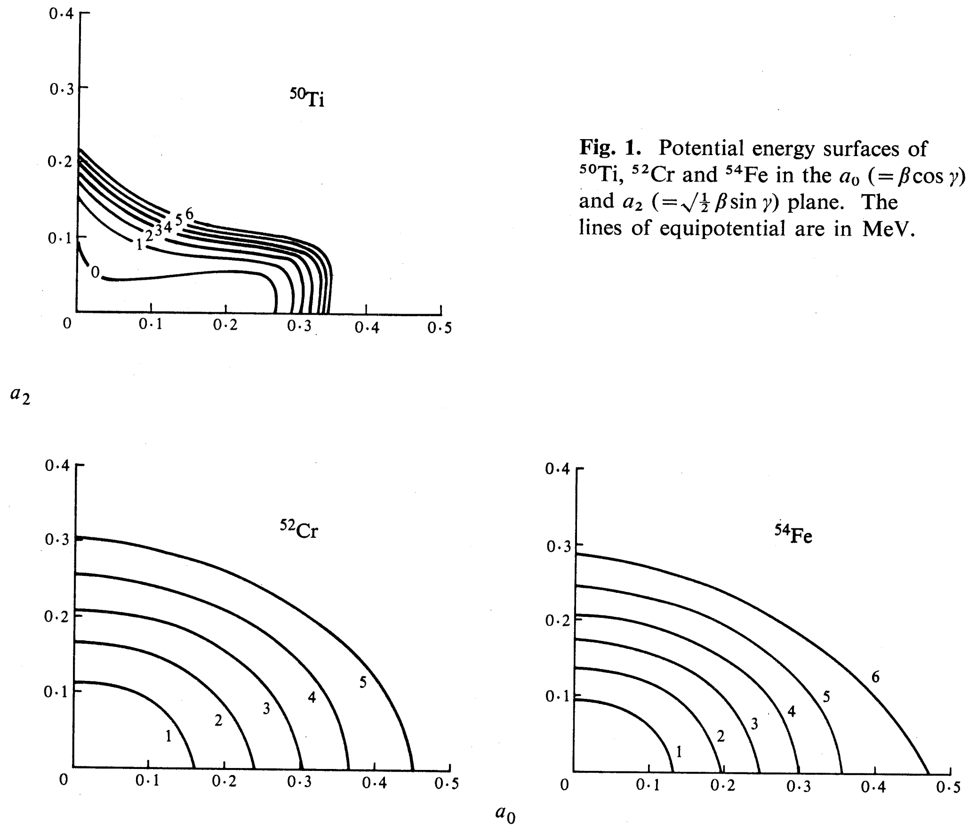

Fig. 1. Potential energy surfaces of ^{50}Ti, ^{52}Cr and ^{54}Fe in the a_0 ($=\beta\cos\gamma$) and a_2 ($=\sqrt{\frac{1}{2}}\beta\sin\gamma$) plane. The lines of equipotential are in MeV.

In Fig. 2 the calculated energy levels, and in Tables 2 and 3 the quadrupole moments and B(E2) transition rates respectively, are compared with the available data. The Gneuss–Greiner model is able to reproduce satisfactorily the low energy spectra of these nuclei and in particular the required lowering of the 0_2^+ states. Although the predicted reduced E2 transition probabilities involving the higher angular momentum states are generally larger than found experimentally, the $2_2^+ \to 0_1^+$ and $2_2^+ \to 2_1^+$ transition strengths compare very well for ^{52}Cr. Obviously the B(E2) transition rates exceed single particle estimates, but it seems the collectivity decreases with increasing angular momentum. The structure of the $J^\pi = 4^+$ and 6^+ levels is best described in terms of $(f_{7/2})^2$ fermion pairs, not of two and three quadrupole phonons. Muther *et al.* (1977) extended the (collective) generator coordinate method (GCM) to include two quasi-particle excitations in an effort to introduce single particle degrees of freedom. The fit for the even–even $N = 28$ isotones was considerably better than with the GCM alone. Similarly in the IBA, it is possible to couple single particle degrees of freedom to phonon excitations (Morrison and Faessler 1981, to be published).

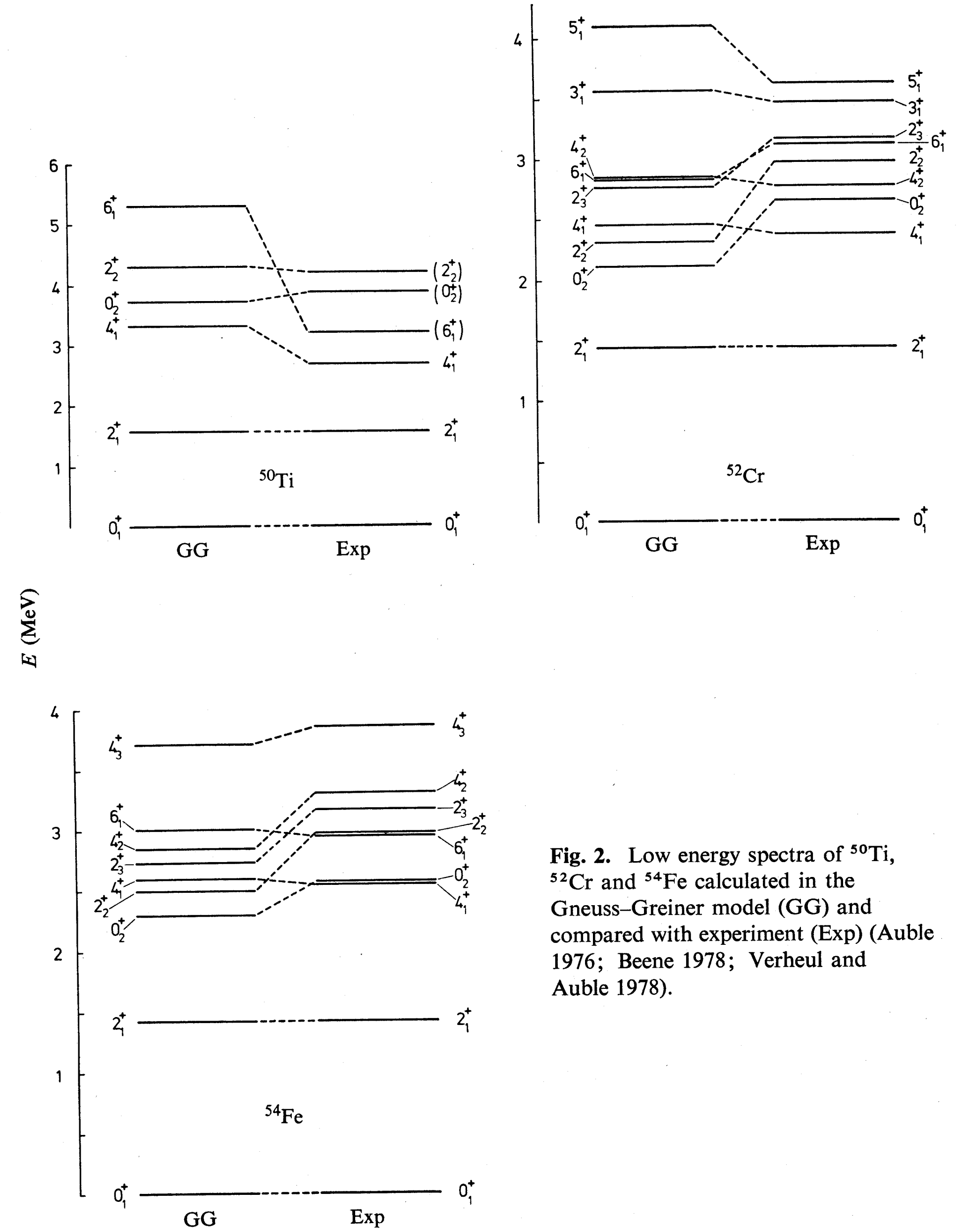

Fig. 2. Low energy spectra of ^{50}Ti, ^{52}Cr and ^{54}Fe calculated in the Gneuss–Greiner model (GG) and compared with experiment (Exp) (Auble 1976; Beene 1978; Verheul and Auble 1978).

The failure of the Gneuss–Greiner model to describe adequately the low energy properties of the higher angular momentum states should not significantly affect the predictions of the model in the GDR region, since only states with angular momenta 0 and 2 enter into the interaction and here specifically the 0_1^+, 2_1^+ states, the features of these comparing favourably with the available experimental data. In Fig. 3, the calculated total absorption cross sections, the experimental data and the positions of the major dipole strengths are presented for ^{50}Ti, ^{52}Cr and ^{54}Fe. The main contributions to the total absorption data comprising the (γ,n) and (γ,p) cross sections are summed in these figures. For ^{54}Fe only the (γ, n) cross section was available and therefore one expects additional strength on the higher energy side of the unperturbed dipole energy $\hbar\omega_1$ due to the (γ, p) contribution. The unperturbed dipole energy $\hbar\omega_1$ and the width of all the dipole strengths Γ_n were taken arbitrarily to be 20·0 and 3·0 MeV respectively so as to match the energy and resolution of the data. In Fig. 4, the calculated (γ, γ') scattering cross sections to the ground state and the first 2^+ state at 135° are presented. The inelastic scattering to the 0_2^+, 2_2^+ and 2_3^+ states was negligible and thus not included. This is consistent with the 0_1^+ and 2_1^+ states being the dominant terms in the GDR calculation.

Table 2. Comparison of calculated quadrupole moments $Q(2_1^+)$ with available data

Units are $e\,\mathrm{fm}^2$

Nucleus	Calculated	Experimental
^{50}Ti	-14	-2 ± 9[A]
^{52}Cr	-6	-14 ± 8[B]
^{54}Fe	-2	

[A] Hausser *et al.* (1970). [B] Brown *et al.* (1974).

Table 3. Comparison of calculated transition probabilities $B(\mathrm{E2}: J_i \to J_f)$ with available data

Units are $e^2\,\mathrm{fm}^4$

Nucleus	$J_i^+ \to J_f^+$	Calc.	Exp.	Nucleus	$J_i^+ \to J_f^+$	Calc.	Exp.
^{50}Ti	$2_1 \to 0_1$	66	66 ± 6[A]	^{54}Fe	$2_1 \to 0_1$	102	102 ± 10[F]
	$4_1 \to 2_1$	131	60 ± 12[B]		$2_2 \to 0_1$	0	$27{\cdot}2 \pm 4{\cdot}5$[G]
	$6_1 \to 4_1$	180	34 ± 1[C]		$2_2 \to 2_1$	94	$5{\cdot}7^{+5{\cdot}1}_{-3{\cdot}7}$[G]
^{52}Cr	$2_1 \to 0_1$	135	132 ± 6[D]		$2_3 \to 0_1$	2	$8{\cdot}8 \pm 1{\cdot}9$[G]
	$2_2 \to 0_1$	0	$< 0{\cdot}2$[D]		$2_3 \to 2_1$	140	$12{\cdot}7^{+20}_{-7{\cdot}8}$[G]
	$2_2 \to 2_1$	107	157 ± 23[D]		$0_2 \to 2_1$	247	$\leqslant 199$[G]
	$4_1 \to 2_1$	194	81 ± 18[D]		$4_1 \to 2_1$	178	78 ± 16[B]
	$4_2 \to 2_1$	139	93 ± 26[D]		$6_1 \to 4_1$	1070	$40 \pm 0{\cdot}5$[B]
	$4_2 \to 4_1$	322	92^{+37}_{-24}[E]				
	$6_1 \to 4_1$	1961	$59{\cdot}5 \pm 3{\cdot}4$[B]				
	$6_1 \to 4_2$	576	$30{\cdot}4 \pm 4{\cdot}5$[B]				

[A] Hausser *et al.* (1970). [B] Brown *et al.* (1974). [C] Cochavi *et al.* (1970); Nomura *et al.* (1970). [D] Towsley *et al.* (1975). [E] Brown (1971). [F] Stelson and Grodzins (1965). [G] Moss *et al.* (1972).

The predicted total absorption cross sections strongly exhibit the features of spherical nuclei. The splitting of the GDR states, however, is much larger than for a harmonic vibrator due to the presence of anharmonicities. If this interpretation is correct, there should be considerable inelastic γ scattering only into the 2_1^+ states (interpreted as the one phonon states) of these nuclei, as is found. The gross features of the experimental absorption cross sections are satisfactorily reproduced although an adequate description of the fine structure on the low energy side of the main dipole strength is not obtained. This is not surprising, however, as such structure has long been associated with single particle excitations. The additional strength found experimentally on the high energy side may be due to the isovector E2 giant resonance predicted to occur at $\approx 1.6\,\hbar\omega_1$.

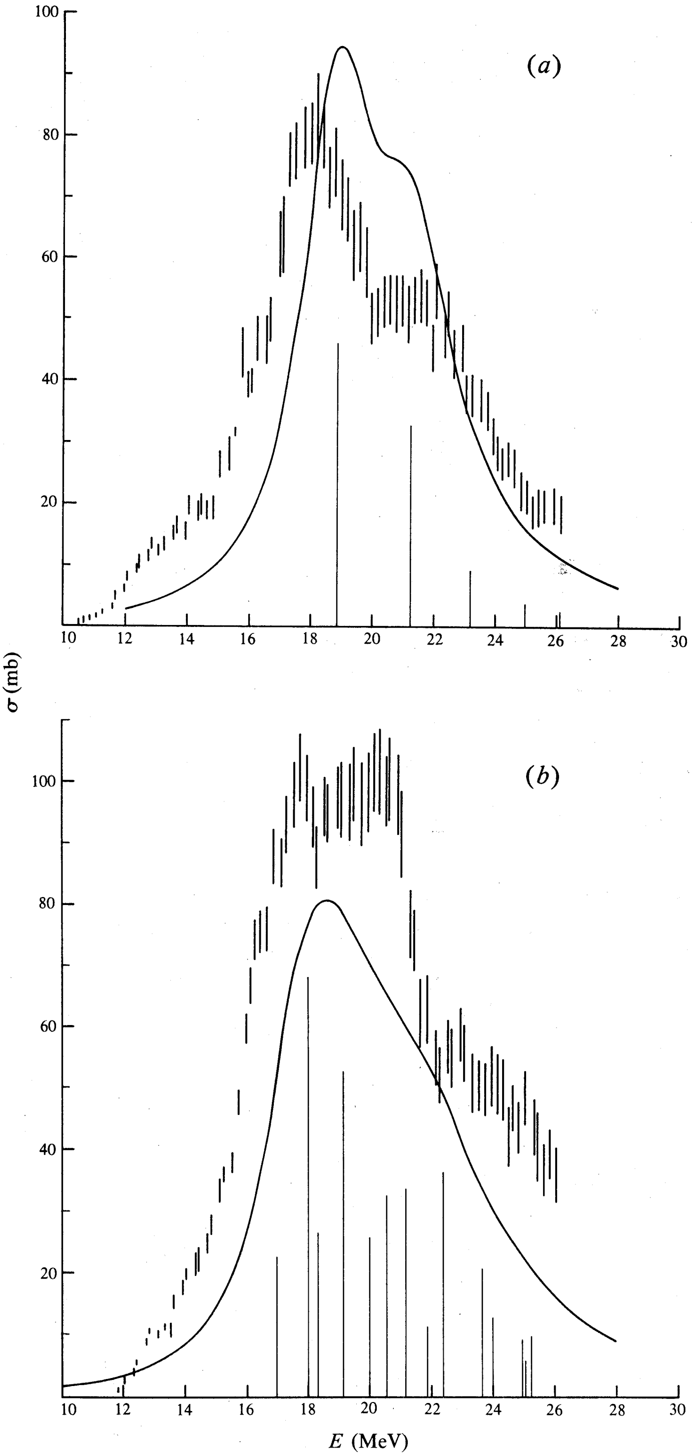

Figs 3*a* and 3*b*. (*See caption on opposite page*)

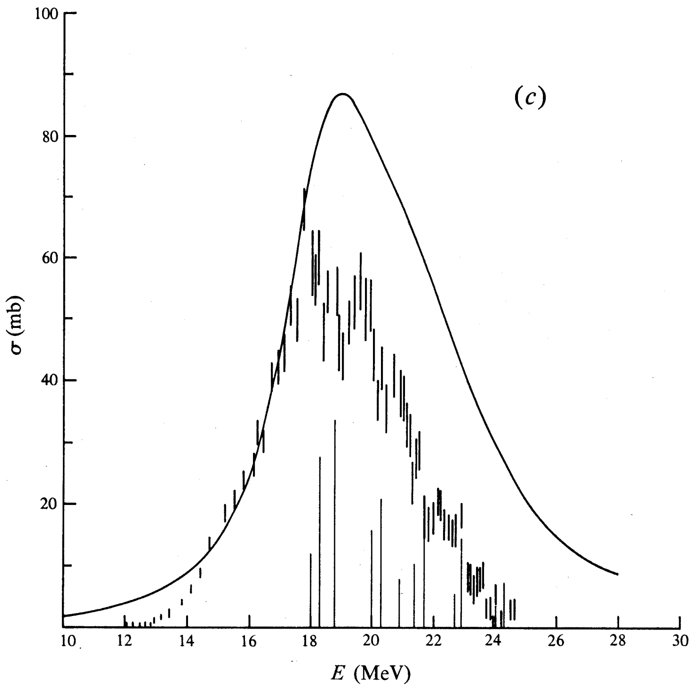

Fig. 3. Calculated and experimental (Pywell *et al.* 1980; Weise *et al.* 1977; Norbury *et al.* 1978) total absorption γ-ray cross sections of (*a*) ^{50}Ti, (*b*) ^{52}Cr and (*c*) ^{54}Fe. Also shown are the major dipole strengths $\langle l_n \| D \| 0 \rangle$.

As shown in Table 4, the measured integrated cross sections compare favourably with the dipole sum rule estimates; any additional strength may be due in part to exchange forces which can increase the classical estimate by as much as 30% of its original value. A comparison of the calculated dipole sum rule with the classical estimate indicates that the contribution from the interaction H_{DQ} is small.

Very few photon scattering data are available in the GDR region. However, Arenhovel and Maison (1970) measured the differential photon scattering cross section to the 0_1^+ and 2_1^+ states of natural chromium at $\theta = 150°$. Although the statistics are not particularly good, a comparison is made with the present model predictions in Fig. 5. The strengths of the elastic and inelastic scattering are under- and over-estimated respectively. Nathan and Morch (1980) recently found such an inadequacy in a DCM calculation of the inelastic scattering to the 2^+ γ band in Er. More precise photon scattering cross section measurements, therefore, should provide an invaluable means of investigating the limitations of this model and perhaps a direction for further development.

Overall, the Gneuss–Greiner model provides a simple collective model description of the GDR structure for the $N = 28$ isotones considered. Since the Hamiltonian of equation (1) essentially contains only contributions from the 0_1^+ and 2_1^+ states in the present calculation, the low energy properties (transition strengths and quadrupole moments) of which are fitted, the predictions in the GDR region merely reflect shape transitions. However, the poor comparison with data of the low energy properties involving higher angular momentum states suggests that non-collective

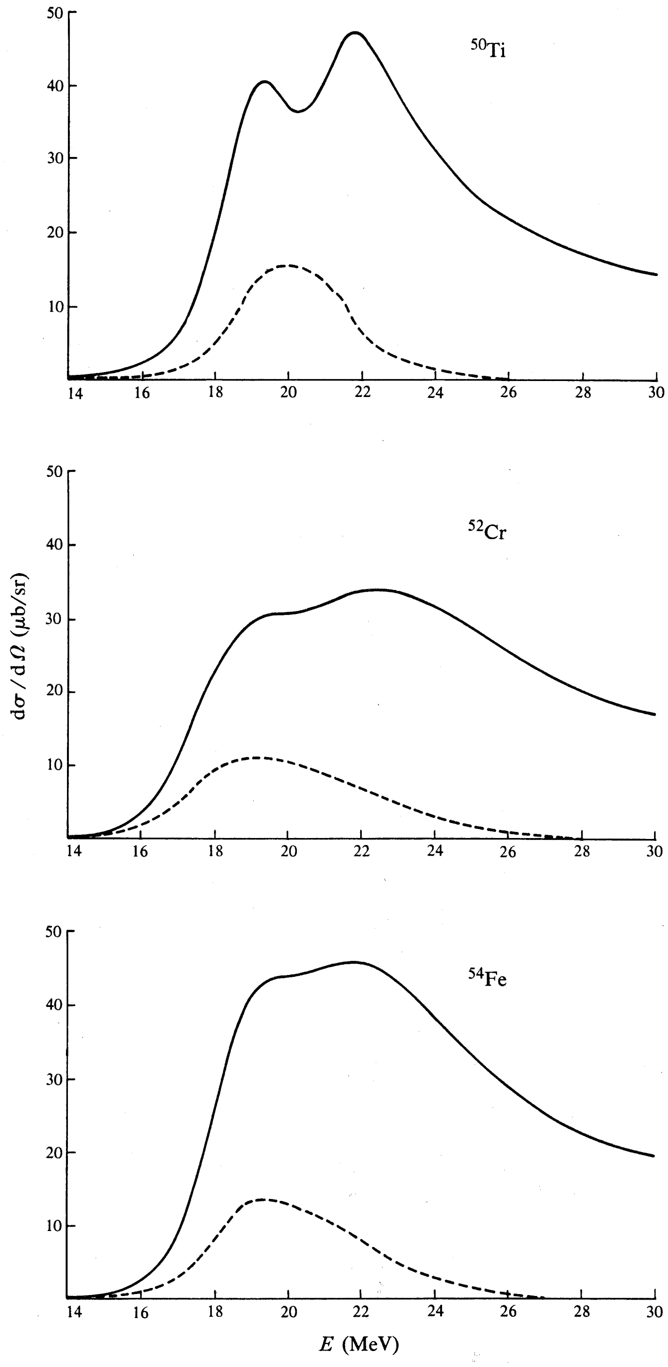

Fig. 4. Calculated differential γ-ray scattering cross sections to the ground state (full curve) and first excited 2^+ state (dashed curve) of ^{50}Ti, ^{52}Cr and ^{54}Fe at $\theta = 135°$.

Table 4. **Comparison of dipole sum rule with integrated cross section and classical estimate**

Nucleus	DSR	Exp	$60NZ/A$
^{50}Ti	654·8	584±57	739·2
^{52}Cr	684·1	860±106	775·4
^{54}Fe	714·1	~320[A]	808·9

[A] Contribution from $\int \sigma(\gamma, n)\, dE$ only.

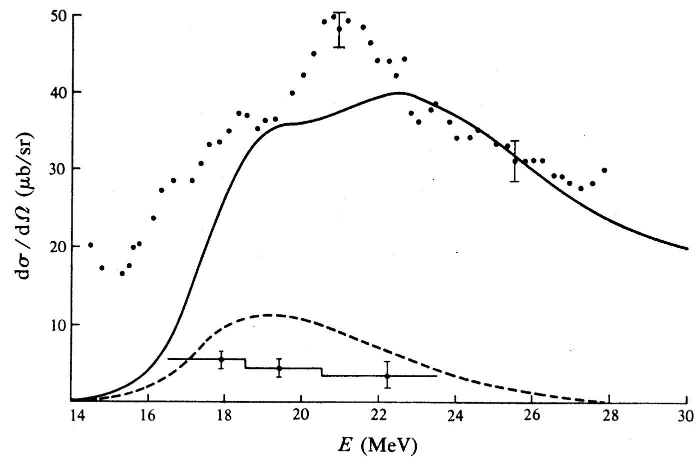

Fig. 5. Experimental (Arenhovel and Maison 1970) and calculated differential scattering cross sections to the ground state (dots and full curve) and 2_1^+ state (histogram and dashed curve) at 150° in ^{52}Cr.

effects are critical in providing a good description of the low energy region. This has been demonstrated, for example, by Kishimoto and Tamura (1976) in the boson expansion theory, where in addition to the collective Hamiltonian, single-particle and fermion-pair degrees of freedom are required to describe satisfactorily low energy features of a range of nuclei.

References

Amos, K., Faessler, A., Morrison, I., Smith, R., and Muther, H. (1978). *Nucl. Phys.* A **304**, 191.
Arenhovel, H., and Maison, J. M. (1970). *Nucl. Phys.* A **147**, 305.
Auble, R. L. (1976). *Nucl. Data Sheets* **19**, 291.
Beene, J. R. (1978). *Nucl. Data Sheets* **25**, 235.
Brown, B. A. (1971). *Phys. Rev.* C **4**, 2074.
Brown, B. A., Fossan, D. B., McDonald, J. M., and Snover, K. A. (1974). *Phys. Rev.* C **9**, 1033.
Cochavi, S., Fossan, D. B., Henson, S. H., Alburger, D. E., and Warburton, E. K. (1970). *Phys. Rev.* C **2**, 2241.
Gneuss, G., and Greiner, W. (1971). *Nucl. Phys.* A **171**, 449.
Hausser, O., Pelte, D., Alexander, T. K., and Evans, H. C. (1970). *Nucl. Phys.* A **150**, 417.
Kishimoto, T., and Tamura, T. (1976). *Nucl. Phys.* A **270**, 317.
Lips, K. (1971). *Phys. Rev.* C **4**, 1482.
Lips, K., and McEllistrem, M. T. (1970). *Phys. Rev.* C **1**, 1009.
Morrison, I., Smith, R., and Amos, K. (1975). *Nucl. Phys.* A **244**, 189.
Morrison, I., and Weise, J. (1981). Dipole states in the interacting boson model. *J. Phys.* G (in press).

Moss, J. M., Heindrie, D. L., Glashausser, C., and Thirion, J. (1972). *Nucl. Phys.* A **194**, 12.
Muther, H., Goeke, K., Allaart, K., and Faessler, A. (1977). *Phys. Rev.* C **15**, 1467.
Nathan, A. M., and Morch, R. (1980). *Phys. Lett.* B **91**, 38.
Nomura, T., Gil, C., Saito, H., Yamazaki, T., and Ishihara, M. (1970). *Phys. Rev. Lett.* **25**, 1342.
Norbury, J. W., Thompson, M. N., Shoda, K., and Tsubota, H. (1978). *Aust. J. Phys.* **31**, 471.
Pronko, J. G., Bardin, T. T., Becker, J. A., McDonald, R. E., and Poletti, A. R. (1974). *Phys. Rev.* C **10**, 1345.
Pywell, R. E., Thompson, M. N., and Hicks, R. A. (1980). *Nucl. Phys.* A **325**, 116.
Rebel, H., and Habs, D. (1973). *Phys. Rev.* C **8**, 1391.
Rezwani, V., Gneuss, G., and Arenhovel, H. (1970). *Phys. Rev. Lett.* **25**, 1667.
Rezwani, V., Gneuss, G., and Arenhovel, H. (1972). *Nucl. Phys.* A **180**, 254.
Saayman, R., and Irvine, J. M. (1976). *J. Phys.* G **2**, 309.
Sedlmayr, R. (1976). Dissertation, Universität Frankfurt am Main.
Stelson, P. H., and Grodzins, L. (1965). *Nucl. Data* A **1**, 21.
Towsley, C. W., Cline, D., and Horoshko, R. N. (1975). *Nucl. Phys.* A **250**, 381.
Verheul, H., and Auble, R. L. (1978). *Nucl. Data Sheets* **23**, 455.
Weise, Jeanette, Thompson, M. N., Shoda, K., and Tsubota, H. (1977). *Aust. J. Phys.* **30**, 401.

Manuscript received 6 August, accepted 2 October 1981